CO and CO_2 dual-gas detection based on mid-infrared wideband absorption spectroscopy*

DONG Ming (董明), **ZHONG Guo-qiang** (钟国强), **MIAO Shu-zhuo** (苗澍茁), **ZHENG Chuan-tao** (郑传涛)**, **and WANG Yi-ding** (王一丁)

State Key Laboratory on Integrated Optoelectronics, College of Electronic Science and Engineering, Jilin University, Changchun 130012, China

(Received 13 November 2017; Revised 7 December 2017)

A dual-gas sensor system is developed for CO and CO_2 detection using a single broadband light source, pyroelectric detectors and time-division multiplexing (TDM) technique. A stepper motor based rotating system and a single-reflection spherical optical mirror are designed and adopted for realizing and enhancing dual-gas detection. Detailed measurements under static detection mode (without rotation) and dynamic mode (with rotation) are performed to study the performance of the sensor system for the two gas samples. The detection period is 7.9 s in one round of detection by scanning the two detectors. Based on an Allan deviation analysis, the 1σ detection limits under static operation are 3.0 parts per million (ppm) in volume and 2.6 ppm for CO and CO_2, respectively, and those under dynamic operation are 9.4 ppm and 10.8 ppm for CO and CO_2, respectively. The reported sensor has potential applications in various fields requiring CO and CO_2 detection such as in the coal mine.

Document code: A **Article ID:** 1673-1905(2018)02-0119-5

DOI https://doi.org/10.1007/s11801-018-7248-1

The development of dual-gas or multi-gas detection technology plays an important role in many areas, such as environmental atmospheric monitoring[1,2], medical diagnosis[3,4], industrial process control[5,6] and fire alarm systems in coal mines[7-10]. So far, the most widely used technology for dual- or multi-gas instruments is photo-acoustic spectroscopy (PAS) and catalytic reaction. PAS detects gas concentration by acquiring acoustic signals in the gas chamber based on photoacoustic principle[11-13]. However, environment vibrations will interfere with normal sensor operation and cause measurement errors of the PAS sensor. A gas sensor based on a catalytic reaction has a much shorter service lifetime compared with infrared (IR) sensors[14,15]. Direct absorption spectroscopy (DAS) has the advantages of compact design and high performance-cost ratio. In addition, a broadband thermal source and pyroelectric detector in a DAS technique are less costly compared with a mid-infrared laser and photovoltaic detector.

The developed sensor is intended to be used in mining industry, where the normal CO and CO_2 concentrations are less than several ppm and hundreds to thousands of ppm, respectively. The detection limits of CO and CO_2 are designed to be <10 ppm and <100 ppm, respectively, to meet the requirements of mining detection. In order to reduce sensor cost, a single broadband light source and double detectors are used in this work to realize a dual-gas sensor based on DAS. The emission spectrum of the wideband light source covers the mid-infrared absorption bands of CO (4.65 μm), and CO_2 (4.26 μm), which are fundamental absorption bands of these two gas samples. A mechanical rotation module is designed to switch between the two gas detectors and the two gases are detected in sequence using time-division multiplexing (TDM) technique. Both static (without rotation) and dynamic (with rotation) detection characteristics are studied.

As shown in Fig.1, the proposed multi-gas sensor system can be divided into optical, mechanical and electrical parts. In the optical part, the light emitted by a broadband light source (Boston Electronics, IR-55, USA) is reflected by a spherical mirror with a focal length of 100 mm and converges at a point which a pyroelectric detector is rotated to. The detector has a reference channel and a detection channel with two different filters installed in the window assembly. The detector will generate a detection signal and a reference signal. In the mechanical part, the supporting frame and disc are simulated

* This work has been supported by the National Key R&D Program of China (Nos.2016YFD0700101 and 2016YFC0303902), the National Natural Science Foundation of China (Nos.61775079, 61627823 and 61307124), the Science and Technology Planning Project of Guangdong Province, China (No.2017A020216011), the Science and Technology Development Program of Jilin Province, China (No.20140307014SF), the Industrial Innovation Program of Jilin Province, China (No.2017C027), and Changchun Municipal Science and Technology Bureau, China (No.14KG022).

** E-mail: zhengchuantao@jlu.edu.cn

by a software tool named unigraphics (UG) and fabricated using 3-D printing technology. The two dual-channel pyroelectric detectors (InfraTec, Germany) with different wavelengths for CO and CO_2 sensing are mounted on a disc with an interval angle of 45°. The disc is driven by a stepper motor. When a detector moves to the light converging point, it will remain at this point for the time required for gas detection. The sensor system switches continuously between the two detectors to detect the two gases, which can then be processed by the TDM technique. In order to improve the accuracy and stability of the rotation system, a 1/8 subdivided motor driver and an incremental encoder are used for feedback of the current angle of the stepper motor to form a closed-loop rotation control system. In the electrical part, a digital signal processor (DSP) reads the current angle from the encoder by means of an enhanced quadrature encoder pulse module (eQEP). A closed-loop algorithm is used to precisely control the rotation and switching of the two detectors. A 4-Hz square-wave signal generated by the DSP by means of an enhanced capture module (eCAP) is used to modulate the broadband light source through a constant current circuit. An analog switch is then used to switch the sensing channels of the two detectors. When a detector starts to operate, it will generate both a detection signal $u_1(\lambda)$ and a reference signal $u_2(\lambda)$. These two signals are first subjected to an impedance match by a preamplifier (PA), which is followed by a differential operation (DA) for generating a differential signal, i.e., $\Delta u(t)=u_2(t)-u_1(t)$. The amplitudes of $u_2(t)$ and $\Delta u(t)$ are then extracted by a custom made lock-in amplifier. The light source modulation signal is used as a reference signal for the lock-in amplifier. The lock-in amplifier will produce a square wave which has the same frequency as the reference signal. The square wave is phase-shifted with respect to the reference signal by the DSP. The signal to be measured and the phase-shifted signal are then multiplied by an analog multiplier after passing through a sampling/holding circuit (S/H) and the output of the multiplier is then fed back to the DSP for sampling. The DSP adjusts the phase difference between the reference and the phase-shift signals according to the feedback and the optimum phase shift obtained with a maximized feedback signal. The output of the lock-in amplifier varies linearly with the amplitude of the sensing signal to be measured. The maximized feedback signal is processed with a sliding average filtering algorithm and finally the results are transmitted to a laptop for real time monitoring.

Fig.2(a) shows the photograph of the optical part of the multi-gas sensor. As the light source has a divergence angle of 15° and the focal length of the spherical mirror is 100 mm, the optical path length can be calculated as the following formulas:

$$\begin{cases} SP = AP \times \cos\angle BAP = f \times \cos 15° = 96.6 \\ SO = SP + PO = 96.6 + 100 = 196.6 \\ AS = AP \times \sin\angle APC = f \times \sin 15° = 25.9 \end{cases} . \quad (1)$$

The optical length is determined to be 393.2 mm, i.e., twice the length of line *SO*.

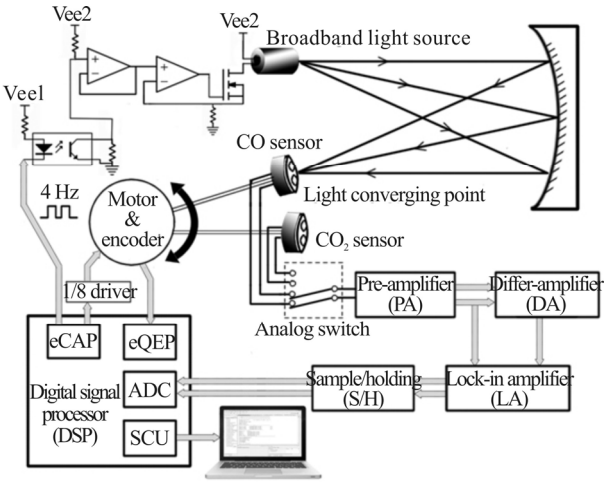

Fig.1 Schematic of the dual-gas sensor system using a broadband light source and two dual-channel pyroelectric detectors

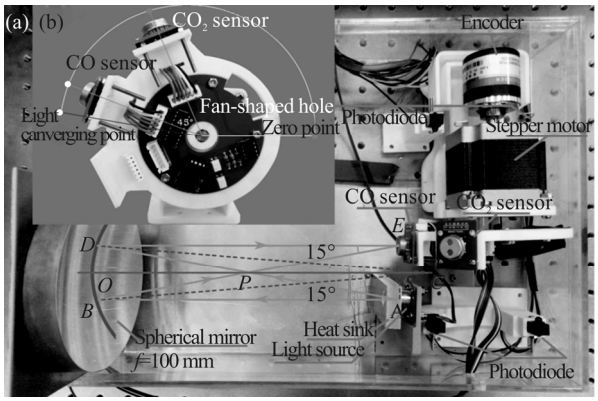

Fig.2 (a) Photograph of the optical part of the dual-gas sensor; (b) Photograph of the disc with a circuit board inlaid and two pyroelectric detectors for the detection of CO and CO_2

The disc is fixed on the front axle of the stepper motor and an incremental encoder is attached on the rear axle of the stepper motor to monitor the rotation. Two pairs of photodiodes are placed on both sides of the motor, where one pair is used to prompt the micro control unit (MCU) when the disc rotates to the zero point of rotation, and the other pair is used to shut down the stepper motor when the software program goes wrong. The optical structure is held by an L-shape aluminum plate. A heat sink is firmly attached to the surface of the light source and fixed to the plate using thermal silica gel, which stabilizes the temperature of the light source and suppresses thermal noise.

As shown in Fig.2(b), the CO and CO_2 detectors are fixed on a disc with signal lines connected to an electric circuit board which is inlaid into the disc. The function of the circuit is to switch the sensing channels of the

detectors and to filter and pre-amplify the sensing signals. The fan-shaped hole on the disc allows the optical signal to transmit between photodiodes. The operating steps of the disc are as follows. Initially, the disc rotates clockwise until the receiver of the photodiodes acquires an optical signal through the hole in the disc. This position of the disc is considered to be the zero point of rotation. The disc rotates by θ counterclockwise so that the CO sensor reaches the light converging point of the mirror (point E in Fig.2(a)) for gas detection. The angle θ is obtained experimentally. Then the disc is rotated by 45° counterclockwise to let the CO_2 sensor reach the light converging point for gas detection. Finally, the disc turns clockwise back to the zero position and starts a new round of dual-gas detection.

By mixing a 5 000 ppm CO and CO_2 sample with 99.999% pure N_2, respectively, the gas samples with different concentration levels are prepared by means of two mass flow meters (Horiba Metron, S49-33/MT, China with a 2% uncertainty).

For calibration, the motor is kept in a static state for only single-gas detection, i.e., the dual-gas sensor is operated without rotation. The dual-gas sensor is put into a good airtight chamber, and two groups of gas experiments are performed with two kinds of gas samples. In each experimental group, a series of gas samples with different concentration levels spaced apart by 100 ppm are prepared and flushed through the chamber. The amplitude of the differential signal (ΔU) and the amplitude from reference channel (U_2) are recorded after sensor readings become stabilized. The measurement results of ΔU and U_2 for a time period of 8 min for each concentration are recorded. In order to eliminate the influence of noise from the light source and the detector of the detection system, we obtain a relationship between $\Delta U/U_2$ and gas concentration C. For CO and CO_2 sensing, the obtained relationship curves between the averaged $\Delta U/U_2$ and the concentration C are shown in Fig.3. The fitting equations of CO and CO_2 are given by Eq.(2) and Eq.(3), respectively, as

$$C = -755.52 \ln\left(\frac{0.47 - \Delta U / U_2}{0.43}\right) , \quad (2)$$

$$C = -912.67 \ln\left(\frac{1.51 - \Delta U / U_2}{1.42}\right) . \quad (3)$$

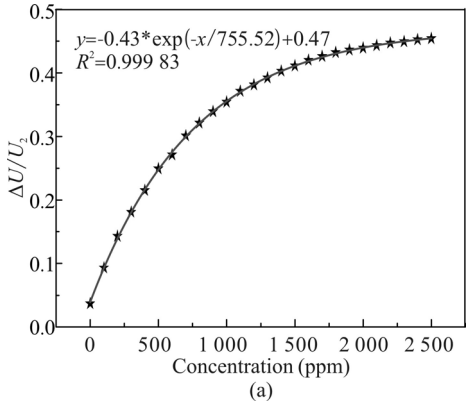

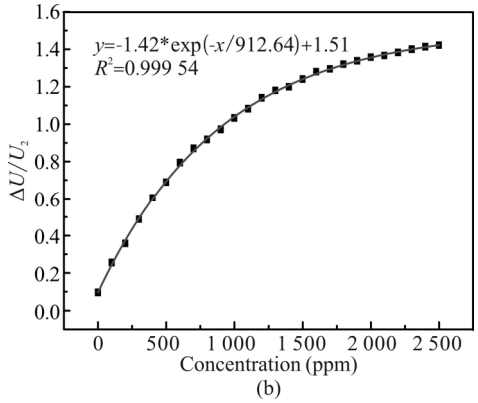

Fig.3 Experimental data dots and fitting curve of the ratio $\Delta U/U_2$ versus concentrations of (a) CO and (b) CO_2

Fig.4 shows the working steps of the dual-gas sensor in one detection cycle. Firstly, the disc rotates clockwise within a time period t_1 (1.25 s) to switch the disc from the CO_2 detection position to the zero point of rotation. After a time delay of t_w (0.5 s), the disc rotates by θ (41°) counterclockwise within a time period t_2 (0.57 s) to let CO detector reach the light converging point of the mirror. After a time delay of t_w for stabilizing, the detector indicates that a measurement time t_D (2 s) is required for signal processing and concentration determination. When the detection of CO is finished, in the same way, the disc will rotate to the CO_2 detection position and detect the gas within a measurement time t_D (2 s). The dual-gas sensor will complete the detection of two gases by scanning the detectors in 7.9 s with a detection time period of 2 s for each gas.

In order to test the stability of the dual-gas sensor, initially, the chamber is flushed by N_2 for 20 min, which is followed by injecting 2% uncertainty 10 mL pure CO and 20 mL pure CO_2 into the chamber. A mixing time period of 20 min is required before detection. Subsequently the dual-gas sensor is operated in a static state without rotation. An experiment is conducted for ~ 5 h for each gas measurement and the results are shown in Fig.5(a). The measured CO concentration varies from 536.85 ppm to 553.88 ppm with an average of 546.23 ± 2.74 ppm (1σ), while the measured CO_2 concentration varies from 852.78 ppm to 875.63 ppm, with an average of 865.72 ± 3.17 ppm (1σ).

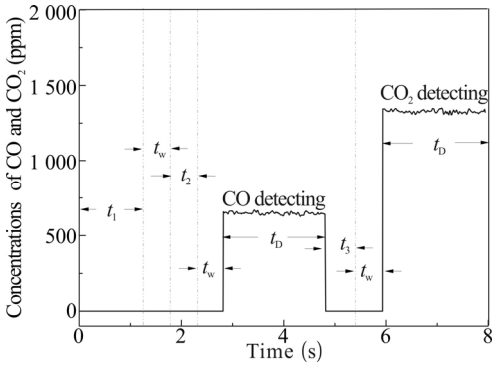

Fig.4 Detection results of two gas samples within a period of 7.9 s based on the dual-gas sensor system

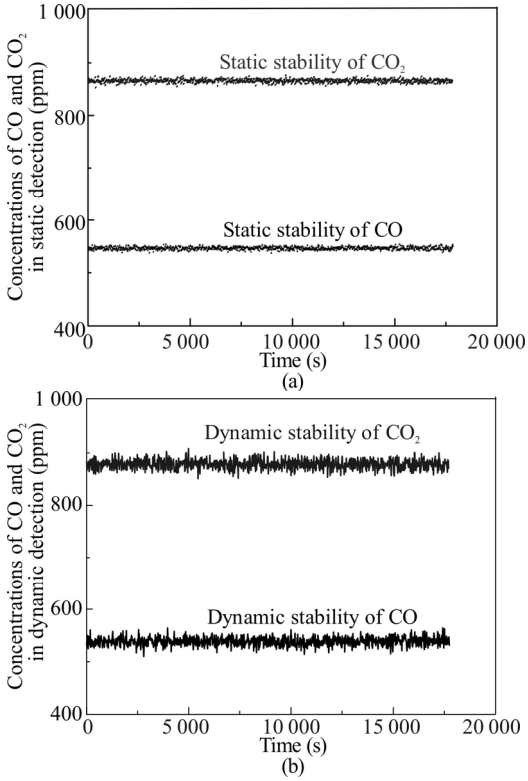

Fig.5 Long-term (a) static and (b) dynamic measurement results of a mixture of CO and CO_2

Based on Fig.6, the Allan deviation for static CO detection is 3.0 ppm with 1 s averaging time, and that for dynamic CO detection is 9.4 ppm with 7.9 s averaging time. Based on Fig.7, the Allan deviation for static CO_2 detection is 2.6 ppm with 1 s averaging time and that for dynamic CO_2 detection is 10.8 ppm with 7.9 s averaging time. So it can be estimated that the 1σ detection limits under static operations are 3.0 ppm and 2.6 ppm for CO and CO_2, respectively, and those under dynamic operations are 9.4 ppm and 10.8 ppm for the two gas samples, respectively. The variation trend of the Allan plot indicates the noise type of the sensor system is related to both hardware and software. Since most of the hardware and software for detecting the two gas samples are the same, the Allan-plot difference among the two gases probably results from the differences among the two pyroelectric detectors.

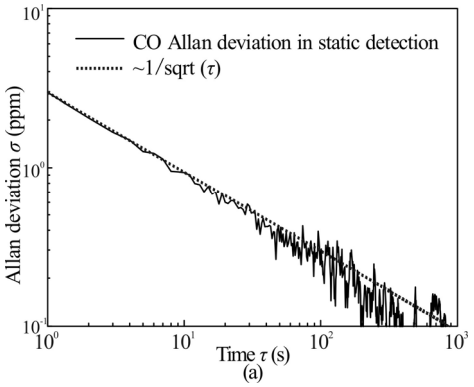

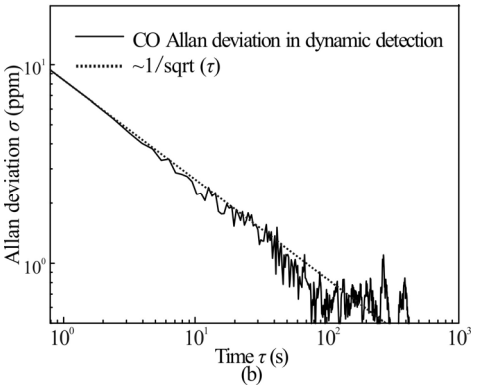

Fig.6 Allan deviation plots of the CO sensor in (a) static state with a sampling interval of 1 s and (b) dynamic state with a sampling interval of 7.9 s

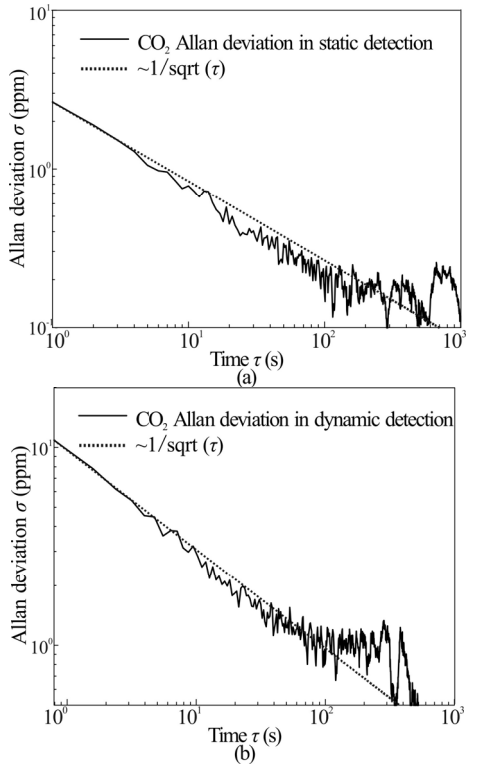

Fig.7 Allan deviation plots of the CO_2 sensor in (a) static state with a sampling interval of 1 s and (b) dynamic state with a sampling interval of 7.9 s

In dynamic detection, the sensor stability is easily affected by the motor vibration during rotation, and the limited resolution of rotation angle for locating gas detectors. Although the motor is driven by a 1/8 subdivided motor driver, slight vibration is inevitable, especially at the moment when the motor suddenly starts or stops. In addition, with an incremental encoder, the angular rotation resolution of the stepper motor is improved from 1.8° to 0.225°. Despite this, there is still positioning error due to a limited resolution of rotation angle for closed-loop control for locating the two detectors. These factors introduce more unknown changes in the detectors' output and thus lead to a decrease of sensor stability compared with static detection without rotation.

In summary, a dual-gas sensor system based on a single broadband light source and two pyroelectric detectors is developed. A stepper motor driven rotation system is designed to switch between the CO and CO_2 detection channels and a single-reflection spherical optical mirror is used to enhance gas absorption. A dual-channel differential detection method is used to suppress noise and improve the detection performance. Both static and dynamic measurements are performed to investigate sensing characteristics of the sensor system. The Allan deviations for static CO and CO_2 detection are 3.0 ppm and 2.6 ppm with 1 s averaging time, respectively, and those for dynamic CO and CO_2 detection are 9.4 ppm and 10.8 ppm with 7.9 s averaging time, respectively. The reported detection method can be applied in various application fields such as the coal mine gas detection.

References

[1] P. Escobedo, M. M. Erenas, N. Lopez-Ruiz, M. A. Carvajal, S. Gonzalez-Chocano, I. de Orbe-Paya, L. F. Capitan-Valley, A. J. Palma and A. Martinez-Olmos, Analytical Chemistry **89**, 1697 (2017).

[2] Yu Lin, Liu Tie-gen, Liu Kun, Jiang Jun-feng and Wang Tao, Sensors & Actuators B Chemical **226**, 170 (2016).

[3] F. Muller, A. Popp, S. Schiller and F. Kuhnemann, SPIE **5**, 138 (2004).

[4] H. Woehlck, M. B. Dunning and K. Nithipatikom, Journal of Clinical Monitoring & Computing **16**, 535 (2000).

[5] U. Banach, C. Tiebe and T. Huebert, Food Control **26**, 23 (2012).

[6] A. Y. Jones and P. K. Lam, Science of the Total Environment **354**, 150 (2006).

[7] D. C. Panigrahi and R. M. Bhattacharjee, Journal-South African Institute of Mining and Metallurgy **104**, 367 (2004).

[8] Jiang Ya-long, Li Gai and Wang Jin-jun, Fire Technology **52**, 1255 (2016).

[9] Xie Zhi-jian and Tan Qiu-lin, International Journal of Infrared & Millimeter Waves **27**, 1639 (2006).

[10] M. C. P. Moura, D. A. C. Branco, G. P. Peters, A. S. Szklo and R. Schaeffer, Energy Policy **61**, 1357 (2013).

[11] H. P. Wu, X. K. Yin, L. Dong, K. L. Pei, A. Sampaolo, P. Patimisco, H. D. Zheng, W. G. Ma, L. Zhang and W. B. Yin, Applied Physics Letters **110**, 121104 (2017).

[12] A. Sampaolo, P. Patimisco, L. Dong, A. Geras, G. Scamarcio, T. Starecki, F. K. Tittel and V. Spagnolo, Applied Physics Letters **107**, 6165 (2015).

[13] F. K. Tittel, A. Sampaolo, P. Patimisco, L. Dong, A. Geras, T. Starecki and V. Spagnolo, Optics Express **24**, A682 (2016).

[14] C. H. Han, D. W. Hong, S. D. Han, J. Gwak and K. C. Singh, Sensors & Actuators B Chemical **125**, 224 (2007).

[15] H. Schwarz, Y. Dong and R. Horn, Chemical Engineering & Technology **39**, 2011 (2016).